3D Printed Soft Robotic Actuator With Embedded Strain Sensing For Position Estimation

Gerjan Wolterink, Stijn Kolkman, Gijs Krijnen
Robotics And Mechatronics group, University of Twente, Enschede, The Netherlands,
Email: gerjan.wolterink@utwente.nl

***Abstract* - This work shows the development and characterization of a fully 3D printed pneumatic soft robotic actuator with embedded strain gauges to estimate the bending angle of the actuator. The actuator was printed in one go using a multi material Fused Filament Fabrication (FFF) printer. By taking the difference of the reading of two integrated strain gauges, printed using carbon doped TPU, a strong linear relation ($R^2 = 0.97$) between the bending angle and sensor output is achieved.**

Keywords - 3D Printing, Sensorized, Soft Actuators, Pneu-net, Strain sensor, Conductive TPU

I. Introduction

Sensorization of soft robotics actuators allows for safe control of soft robots and enables (co)-operating in proximity to humans. Information about the soft robotic's interaction forces with the environment allows e.g. for the development of haptic feedback for tele-operation. Furthermore, sensorized soft robotic actuators may provide real-time information about the deformation of the soft robot to update its control strategy [1].

A common type of soft robotic actuators are the so called "pneu-nets", actuated by pressurizing a network of elastic chambers [2]. 3D printing these soft robotic actuators increases the design freedom, allowing for highly customizable functional structures and automation of the process, eliminating the need for the manual fabrication using molds [3]–[5].

The emerging development of 3D printing technologies and materials facilitates the creation of soft and flexible sensors that can be integrated into functional structures [6], [7]. Elgeneidy et al. [4] have presented a fully FDM printable soft actuator based on a pneu-net design with an embedded strain sensor to provide bending and simple contact feedback. Although both the sensor and the actuator are fully 3D printed there was still a manual fabrication step to combine the sensor with the actuator. Furthermore, the use of a single strain sensor resulted in high hysteresis. This may be expected since soft polymer 3D printed strain sensors commonly show strong non-linear behavior [7]. These effects can be highly reduced by taking the differential signal of two oppositely positioned strain gauges [8]. Therefore, this work introduces and characterizes a fully 3D printed sensorized pneumatic soft robotic actuator with two integrated strain gauges printed in one go using a multi-material FFF 3D printer.

This work was supported by the Dutch Soft Robotics Consortium of the 4TU Federation.

II. Methodology

A. Actuator design

The actuator design was based on a pneu-net design by Mosadegh et al. [2], [9] and was further optimized for fabrication using an FFF 3D printer (see Figure 1). The total size of the actuator was $107.6 \times 14.4 \times 18.8$ mm ($L \times W \times H$). The actuator consists of 11 chambers with an inner dimension of $6.4 \times 11.2 \times 15.4$ mm. The wall thickness was $1.6\,\mathrm{mm}$ and $0.8\,\mathrm{mm}$ between the chamber to increase bending of the actuator. The bottom part of the actuator is $1.8\,\mathrm{mm}$ thick and contains the two strain gauges, one at the top and one at the bottom. Each strain gauge is $0.6\,\mathrm{mm}$ thick (4 layers), has a width of $1.6\,\mathrm{mm}$ (4 traxels) and circumferences the outside of the bottom part of the actuator. The left corner of Figure 1 shows the definition of the bending angle (θ) of the actuator.

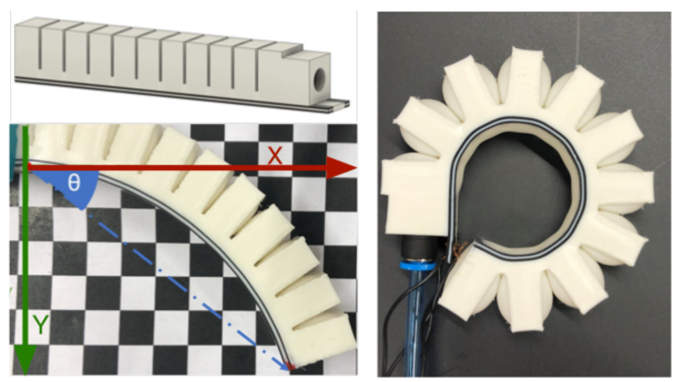

Fig. 1. Top left: CAD model of the actuator. The two black lines are the strain gauges. Bottom left: Definition of the bending angle (θ). Right: Actuator in its maximal bending state ($P \approx 0.6\,\mathrm{MPa}$).

B. Fabrication

The model was sliced (Simplify 3D, Inc., USA) in layers of $0.150\,\mathrm{mm}$ with 3 perimeters. The actuators are printed in one go using a multi-material 3D printer (Diabase H-Series Hybrid, Diabase Engineering, USA) fitted with $0.4\,\mathrm{mm}$ nozzles (Bondtech LGX, Bondtech AB, Sweden). No support was used in the overhangs due to the relative small distance of maximal $11.2\,\mathrm{mm}$. The base material of the actuator is non-conductive thermoplastic polyurethane (TPU) (NinjaFlex

2022 IEEE Sensors | 978-1-6654-8464-0/22/$31.00 ©2022 IEEE | DOI: 10.1109/SENSORS52175.2022.9967233

SemiFlex, Fenner Drives, USA) and the strain gauges are fabricated using a carbon black infused TPU (PI-ETPU 85-700+, Palmiga Innovation, Sweden). Connections to the strain gauges are made by melting in a fine stranded wire. The pneumatic connection is made using a push connection (FESTO Cartridge QSPK10-4).

C. Characterization

The pressure to the actuator is provided using the Soft Robotics Control Unit developed by Caasenbrood et al. [10]. This system consists of a custom-made shield placed on a Raspberry Pi 4 that is connected to a proportional pressure regulator (Festo, VEAB-L-26-D13-Q4- V1-1R1). The Raspberry Pi communicates with a PC running a Simulink (Mathworks Inc., USA) interface to set the pressure. The strain gauges were individually connected in a quarter bridge configuration comparable to [11], of which the voltage was measured using an instrumentation amplifier (AD620, Analog Devices, USA). Subsequently this data is logged using a digital oscilloscope (Handyscope HS5, TiePie engineering, The Netherlands). The same oscilloscopes were also used to log the pressure sensor of the pressure regulator and to blink an LED. This blinking LED was used to synchronize a video (captured at $60\,\mathrm{Hz}$) taken of the actuator with the recording of the scope. Using motion analysis software (Kinovea) the bending angle (as indicated in Figure 1) is obtained.

To analyze the bending angle of the actuator with respect to the pressure, the actuator was pressurized using a triangular wave (0-$0.1\,\mathrm{MPa}$, at $3\,\mathrm{rad\,s^{-1}}$) for 6 cycles. The first cycle was removed from the data set since the slope of the applied pressure deviates from the other five cycles. The force was measured using a load cell (LCMFD-50N, Omega Engineering, USA) positioned under the actuator tip. This load cell was connected to the USB oscilloscope via a load-cell amplifier (IAA100, Futek, USA). The force was measured from $0\,\mathrm{MPa}$ to $0.3\,\mathrm{MPa}$ at angles of $30°$ and $45°$. The data of the strain gauges was low pass filtered at $8\,\mathrm{Hz}$using the Matlab filter function. Subsequently, $\Delta R/R$ was determined using the initial resistance of the strain gauges.

III. Results

Figure 2 shows the correlation between the input pressure and the angle of the actuator for a triangular wave with an amplitude of $0.1\,\mathrm{MPa}$ and a period of $3\,\mathrm{rad\,s^{-1}}$ and for the situation in which there is no load. The force of the actuator at a static position with respect to the pressure is shown in Figure 3. The tip force of the actuator shows a reasonable linear relation with the applied pressure. However, the amount of force decreases with increasing bending angle.

The resistance of the 3D printed strain sensors are $5.01\,\mathrm{k\Omega}$ for the top (CH1) and $7.80\,\mathrm{k\Omega}$ for the bottom (CH2) sensor. The responses of these sensors over time to the bending angle are shown in Figure 4. The relative resistance change versus the angle over multiple periods is shown in Figure 5. The top sensor shows a strong drop in resistance especially after $20°$, the bottom sensor show a strong increase in resistance till

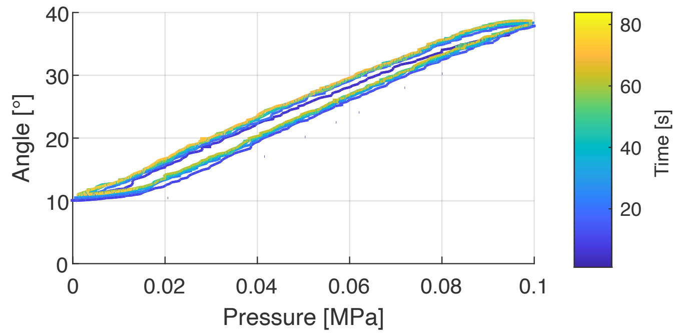

Fig. 2. Actuator angle over pressure, triangular wave input of $3\,\mathrm{rad\,s^{-1}}$.

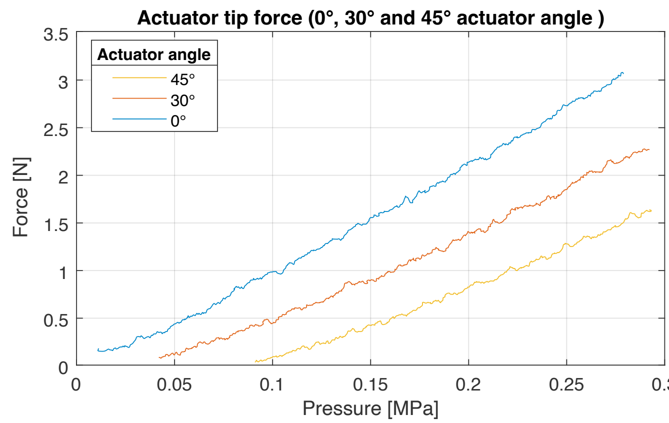

Fig. 3. Actuator output force (measured at the tip) over input pressure.

approximately $25°$ followed by a slow decline in resistance. The difference between the two sensors, shown in the bottom graph of Figure 5, shows a more linear relationship and less hysteresis with respect to the bending angle.

Figure 6 shows that force applied by the tip of the actuator decreases with increasing bending angle. The differential signal of the two strain gauges decreases with increasing force till $2.5\,\mathrm{N}$ after which a strong increase is visible in the $0°$ position. The sensor output decreases with increasing force in the $30°$ situation but increases when the actuator is in a static $45°$ angle.

IV. Discussion

The 3D printed soft robotic actuator shows some air leaks as shown in Figure **??**. However, these leaks are small enough to be compensated by the air flow. The leaks are mainly present around the pneumatic connector and at the two perimeter wide parts of the pneumatic chamber. Further optimizing the printing process and pattern might overcome these issues [3]. The first loop of the bending angle versus the actuator pressure (Figure 2) shows a lower bending angle with respect to the subsequent load cycles.

Although the actuator tip is kept at constant position while determining the actuator force (Figure 3) the actuator was still able to deform due to the applied force. In e.g. the $0°$ angle situation this resulted in an S-shaped curvature of the actuator

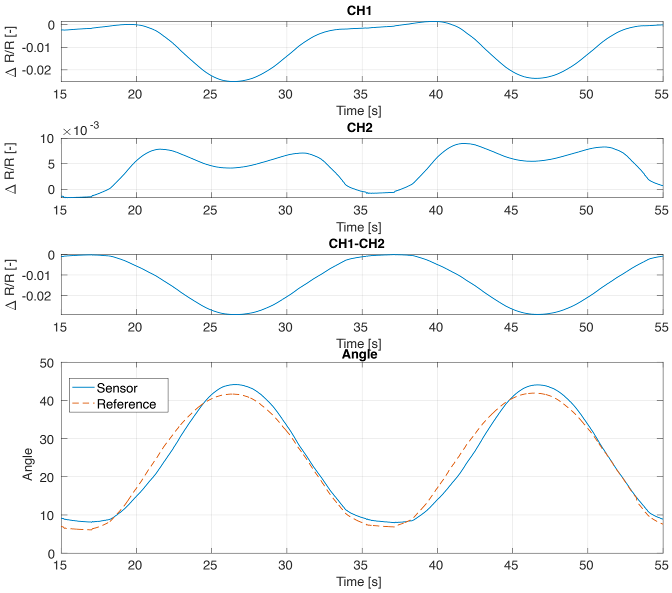

Fig. 4. Relative resistance change of CH1, CH2, CH1-CH2, angle of actuator over time estimated using a linear fit on CH1-CH2 and reference angle.

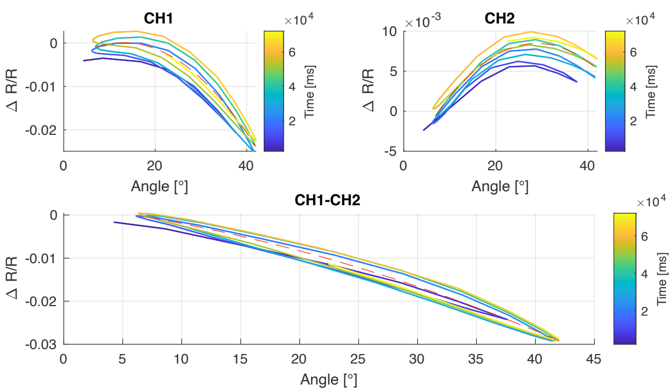

Fig. 5. Relative resistance change of the top (CH1) bottom (CH2) and difference (CH1-CH2) of the strain gauges with respect to the bending angle.

and the associated strain. Furthermore, the total length of the actuator might increase with increasing pressure.

Using carbon doped TPU materials as piezoresistive sensing material comes at the cost of many non-linearities due to viscoelastic properties and physical processes in the matrix of the composite material [11]. However, as expected the differential signal between the bottom and top sensor results in a more linear relative resistance change versus bending angle relationship [8]. Additional compensation algorithms might be used to further improve linearity and limit hysteresis [7], [12].

For the sensing part the actuator can be roughly approximated by a cantilever beam with strain gauges placed below and above the neutral axis. Therefore, the top part will be extended and the bottom part compressed during bending. Carbon doped TPU materials typically show first a strong decline of the resistivity at low strain (< 0.25) followed by an increase of the resistivity [11]. The top sensor in Figure 5 shows this decline indicating low strains due to extension of the sensor. The bottom shows an increase due to compression since this sensor is placed below the neutral axis.

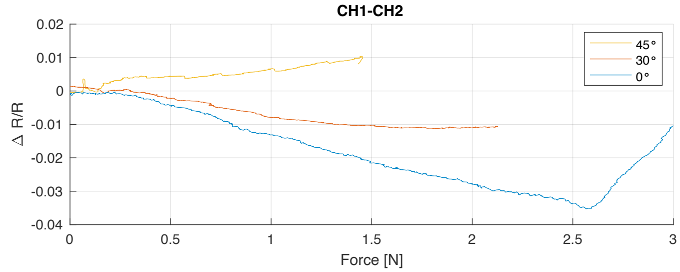

Fig. 6. Actuator output force and the differential resistance change in 30° and 45° position.

The sudden increase of the differential signal of the two strain gauges after 2.5 N in the 0° position, as shown in Figure 6, might also be the result of the same effect on the resistivity of carbon doped TPU at low strain. In the 45° position the strain gauges might be pre-strained to such an extent that only an increase in resistance is shown.

The differential signal of the strain gauges shows a strong linear relation ($R^2 = 0.97$) when there are no external forces acting on the actuator.

This work shows the feasibility to fabricated soft robotics actuators with embedded sensing in one go using FDM 3D printing technologies. The design could be optimized to improve the bending angle and provide the highest sensitivity at angles of most interest for specific applications. Future research is needed to study the effect of the expected cross talk of external forces and if, potentially with the placement of more strain gauges, the bending angle and interaction forces could be estimated [13]. More accurate models predicting the bending of the actuator might help to better understand the strain in the sensing structures. Coupling such models with the feedback of the actuator position might provide the mismatch between the expected and actual position potentially allowing for interaction force prediction. Embedding sensors will potentially result in improved feedback controlled actuators increasingly enabling safe control of soft robots and (co)-operation with humans.

V. Conclusions

This works shows a working concept of a 3D printed soft robotic actuator with embedded sensing that is printed in one go. By taking the differential signal of the two embedded strain gauges a strong linear relation ($R^2 = 0.97$) can be achieved in a bending angle ranging from 5° to 45° with no external load on the actuator.

Acknowledgment

The authors would like to thank Femke van Beek, Chu Khanh Hoang and Brandon Caasenbrood for the development and their support of the Soft Robotics Control Unit.

References

[1] K. Elgeneidy, N. Lohse, and M. Jackson, "Bending angle prediction and control of soft pneumatic actuators with embedded flex sensors – A data-driven approach," *Mechatronics*, vol. 50, no. October 2017, pp. 234–247, 2018. [Online]. Available: https://doi.org/10.1016/j.mechatronics.2017.10.005

[2] B. Mosadegh, P. Polygerinos, C. Keplinger, S. Wennstedt, R. F. Shepherd, U. Gupta, J. Shim, K. Bertoldi, C. J. Walsh, and G. M. Whitesides, "Pneumatic networks for soft robotics that actuate rapidly," *Advanced Functional Materials*, vol. 24, no. 15, pp. 2163–2170, 2014.

[3] G. Stano, L. Arleo, and G. Percoco, "Additive manufacturing for soft robotics: Design and fabrication of airtight, monolithic bending PneuNets with embedded air connectors," *Micromachines*, vol. 11, no. 5, 2020.

[4] K. Elgeneidy, G. Neumann, M. Jackson, and N. Lohse, "Directly printable flexible strain sensors for bending and contact feedback of soft actuators," *Frontiers Robotics AI*, vol. 5, no. FEB, pp. 1–14, 2018.

[5] M. Manns, J. Morales, and P. Frohn, "Additive manufacturing of silicon based PneuNets as soft robotic actuators," *Procedia CIRP*, vol. 72, pp. 328–333, 2018. [Online]. Available: https://doi.org/10.1016/j.procir.2018.03.186

[6] M. Schouten, G. Wolterink, A. Dijkshoorn, D. Kosmas, S. Stramigioli, and G. Krijnen, "A Review of Extrusion-Based 3D Printing for the Fabrication of Electro-and Biomechanical Sensors," *IEEE Sensors Journal*, no. AUGUST, pp. 1–12, 2020.

[7] G. Wolterink, D. Kosmas, M. Schouten, B. J. Van Beijnum, P. Veltink, and G. Krijnen, "Evaluation of A 3D Printed Soft Sensor for Measuring Fingertip Interaction Forces," *IEEE Sensors Journal*, vol. 22, no. 12, pp. 11 499–11 508, 2022.

[8] M. Schouten, B. Prakken, R. Sanders, and G. Krijnen, "Linearisation of a 3D printed flexible tactile sensor based on piezoresistive sensing," *Proceedings of IEEE Sensors*, vol. 2019-Octob, pp. 2019–2022, 2019.

[9] Harvard Biodesign Lab, "Soft Robotics Toolkit," 2018. [Online]. Available: https://softroboticstoolkit.com/

[10] B. J. Caasenbrood, F. E. Van Beek, H. K. Chu, and I. A. Kuling, "A Desktop-sized Platform for Real-time Control Applications of Pneumatic Soft Robots," *2022 IEEE 5th International Conference on Soft Robotics, RoboSoft 2022*, pp. 217–223, 2022.

[11] G. Wolterink, R. Sanders, B.-J. B. J. van Beijnum, P. Veltink, and G. Krijnen, "A 3d-printed soft fingertip sensor for providing information about normal and shear components of interaction forces," *Sensors*, vol. 21, no. 13, pp. 1–13, jul 2021.

[12] D. Kosmas, M. Schouten, and G. Krijnen, "Hysteresis Compensation of 3D Printed Sensors by a Power Law Model with Reduced Parameters," in *FLEPS 2020 - IEEE International Conference on Flexible and Printable Sensors and Systems, Proceedings*, 2020.

[13] T. Pinto, L. Cai, C. Wang, and X. Tan, "CNT-based sensor arrays for local strain measurements in soft pneumatic actuators," *International Journal of Intelligent Robotics and Applications*, vol. 1, no. 2, pp. 157–166, 2017.